

Ductile failure in high-strength steel is a complex process that occurs over different length and time scales. From a modeling viewpoint, it is still impossible to represent all the microstructural features such as dislocations, and primary and secondary inclusions within a single simulation.^{14,15} To overcome this constraint, multiscale techniques such as the hierarchical method^{11,16} described schematically in Figure 1 are used. In short, this method is a bottom-up approach

that consists of homogenizing material properties step by step, from lower to higher scales. At each scale of interest, the microstructure is represented by its

MODELING OF THE MICROSTRUCTURE

It is well known that particular microstructural features can have significant effects on the macro-scale deformation and failure properties of materials. In the case of modern high-strength steels, the relevant microstructure can typically be idealized as consisting of three phases: the matrix material, a population of primary inclusion particles at the micrometer scale, and a population of secondary particles (typically grain refining) ranging between tens and hundreds of nanometers. For each of these phases, a large body of experimental data has been gathered, such as, for example, particle size, volume fraction, spatial distribution, and morphology. As each of these features can become critical to the macroscopic properties, an accurate and faithful modeling of the microstructure is necessary.

M c c e Ge e a d D b

It is known that the inherent randomness in the distributions of particle size, shape, and spatial locations plays a major role in the ductile failure of alloys and must therefore be accounted for in modeling. For instance, Y. Huang³ and M.N. Shabrov⁴ showed that plastic flow localization depends on the location of particle clusters and the intra-cluster particle average spacing. Hence, in the modeling of high-strength steel, it is of crucial importance to base the computations on a distribution and geometric representation of the critical ductility-limiting microstructural features that are faithful to those of the microstructure. However, an accurate modeling of the microstructural details is often computationally prohibitive. Therefore, in this paper the approach consists of starting with a simplified microstructural description and moving toward more complex and accurate models.

The main failure mechanisms in high-strength steels are generally attributed to the nucleation, growth, and coalescence of voids and microvoids around primary and secondary particles, respectively. As failure often begins at the microstructure's weakest point, clusters of particles are known to be the most likely locations for failure initiation. For this reason, in this study, the modeling of the microstructure is performed for clusters in which the local particle density is higher than the average value found in larger sampling domains.

Ma e a P e e P a e

In order to capture the essential physics governing the ductile fracture of steel, it is necessary to utilize the best representation possible for the material properties of the

various features. A major issue is that at small scales, the behavior of materials and their interactions with other phases may become very complex and require the use of small-scale methods such as molecular dynamics. However, such methods are restricted to relatively small computational domains and therefore cannot be used for domains which comprise one or several secondary particles. Thus, this study mainly remains in the context of continuum mechanics, employing interfacial properties derived from atomistic modeling.

In the present work, two constitutive models were investigated for the matrix material for which the respective uniaxial stress-strain responses are depicted in Figure A. The first is represented by a linear hardening J2 flow plasticity, based on experimental behavior of a well-studied high-strength modified 4330 steel.⁵ Corresponding material constants are given in Table A. Because the hardening remains constant regardless of the level of strain, this model can be considered an upper bound of the real matrix material behavior when extrapolated to high strains. The second model is based on an internal state variable formulation.⁶ Here, a simple isotropic hardening model is used to represent the alloy matrix. The evolution equation for the isotropic hardening strength is motivated from dislocation mechanics, and both dislocation hardening and dynamic recoveries are accounted for. Dislocation hardening refers to dislocation-dislocation impedance. Dynamic recovery may be caused by dislocation cross slip. The yield function is simply stated in Equation 1 (all equations are shown in the Equations table), where $\|\sigma^{dev}\|$ is the tensor norm of the deviatoric Cauchy stress (see Equation 2), κ ; initial value $\kappa = 0$ is the isotropic hardening strength; and Y is the initial yield strength. The evolution equation for the isotropic hardening is given by

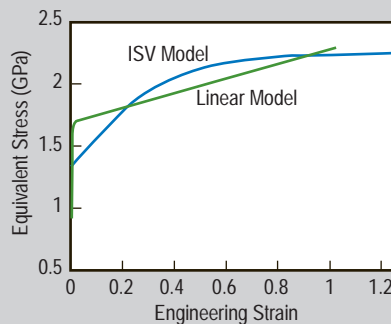


Figure A. A comparison of the tensile stress-strain response of the internal state variable model (ISV) and the linear hardening 4330mod steel model.

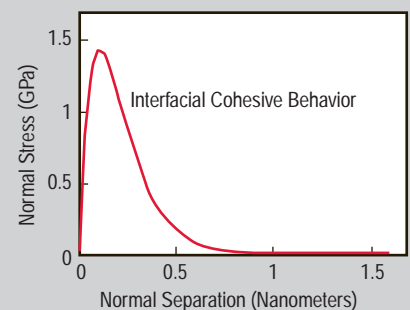


Figure B. A typical force-separation curve at the particle-matrix interface, used at the continuum scale.

Equation 3, where H is the hardening modulus, $\|D^p\|$ is the tensor norm of the rate of plastic deformation (see Equation 4), and R_d is the dynamic recovery modulus. This results in a saturation stress being reached where the rate of hardening is equal to the rate of recovery, and the tensor norm of the Cauchy stress deviator remains on a plateau. At the sub-micrometer scale of interparticle matrix ligaments, one can expect scale-dependent effects based on discrete dislocation interactions to play increasingly important roles in local deformation and failure processes, suggesting the desirability of matrix plasticity models based on nonlocal, strain-gradient, or polarized dislocation density flux theories.⁷⁻⁹ For now, such scale-dependent matrix plasticity models are not considered.

Material models for primary and secondary particles are based on the properties of titanium nitride and titanium carbide, respectively. Nucleation of voids from particles can occur either through cracking of the particles or from decohesion at the particle-matrix interface. In this study, small, strong, equiaxed particles are considered, and therefore cracking is not very likely. Hence, the particles are considered as perfectly elastic, with a high elastic modulus, consistent with experimental data on titanium carbide and titanium nitride. The material constants used in this paper are summarized in Table A, where E denotes the Young's modulus, ν is the Poisson's ratio, H is the hardening modulus, and Y the yield stress.

Finally, the finite-element method was used for material modeling. In this paper, the simulations were performed with the commercial software *ABAQUS/Explicit*[®].

Debonding at Particle-Matrix Interface

The macroscopic fracture of steel often starts with decohesion between particles and the alloy matrix. The interfacial debonding energy and cohesive strength at the iron-carbide interface (Fe-TiC) for secondary particles and iron-nitride (Fe-TiN) for primary particles are therefore major parameters in the fracture process. The determination of the bonding energy between TiC and iron was first performed by Freeman and co-workers¹⁰

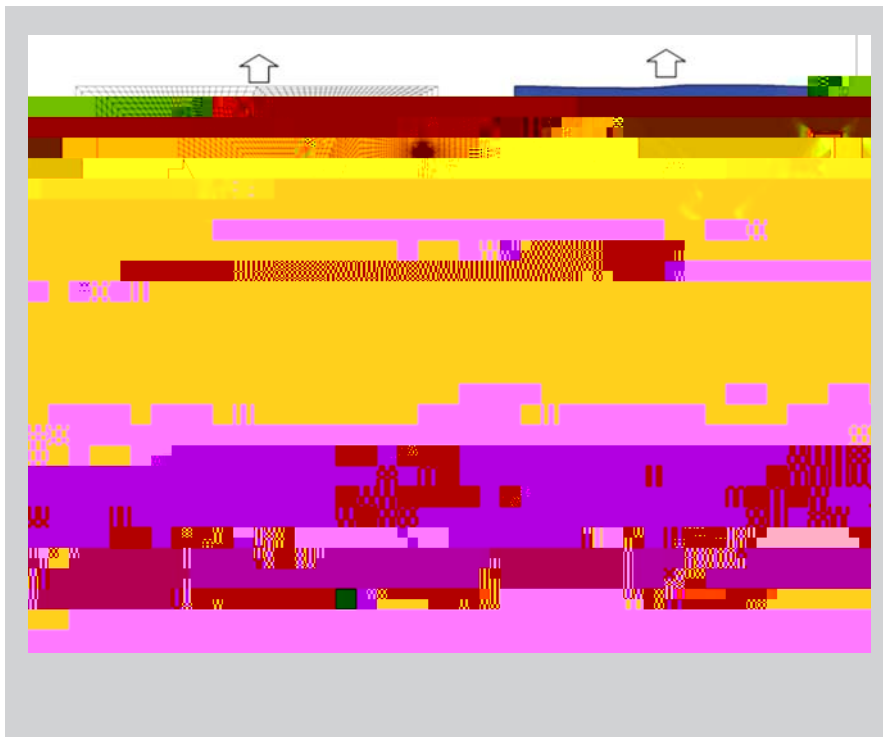
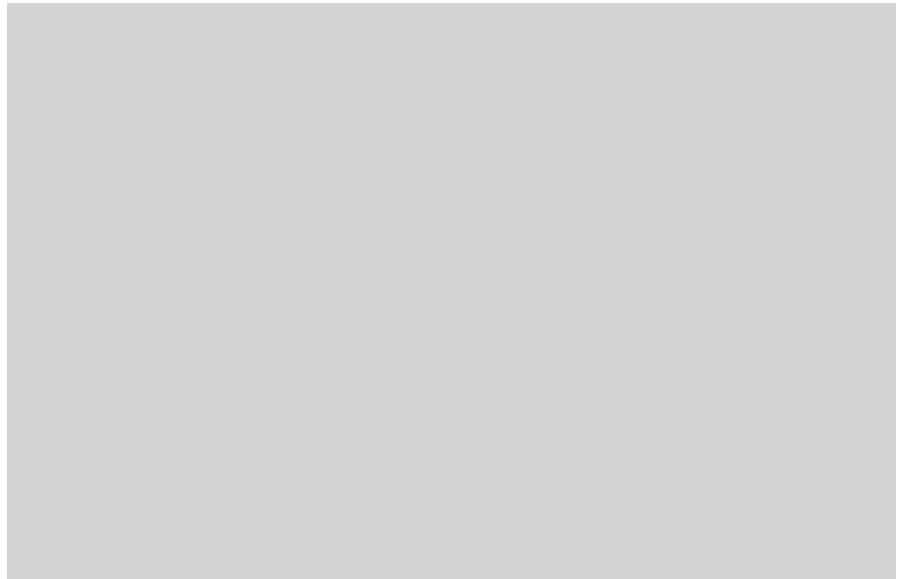
literature.^{6,20} Generally, three main stages can be observed: nucleation of cavities from primary particles, void growth, and failure of the material by a microvoid sheet nucleated from secondary particles. The formation of a microvoid sheet corresponds to the nucleation, growth, and coalescence of microvoids at the site of secondary particles. Figure 2 shows the evolution of equivalent plastic strain from a simulation in which two cuboidal primary particles (TiN) are modeled explicitly, and (effects of) secondary particles are modeled through a homogenized damage model accounting for nucleation, growth, and coalescence of microvoids. The last frame depicts the formation of a microvoid sheet at 45 degrees that is triggered by the interaction between the voids nucleated from the primary particles and microvoids nucleated from secondary particles.

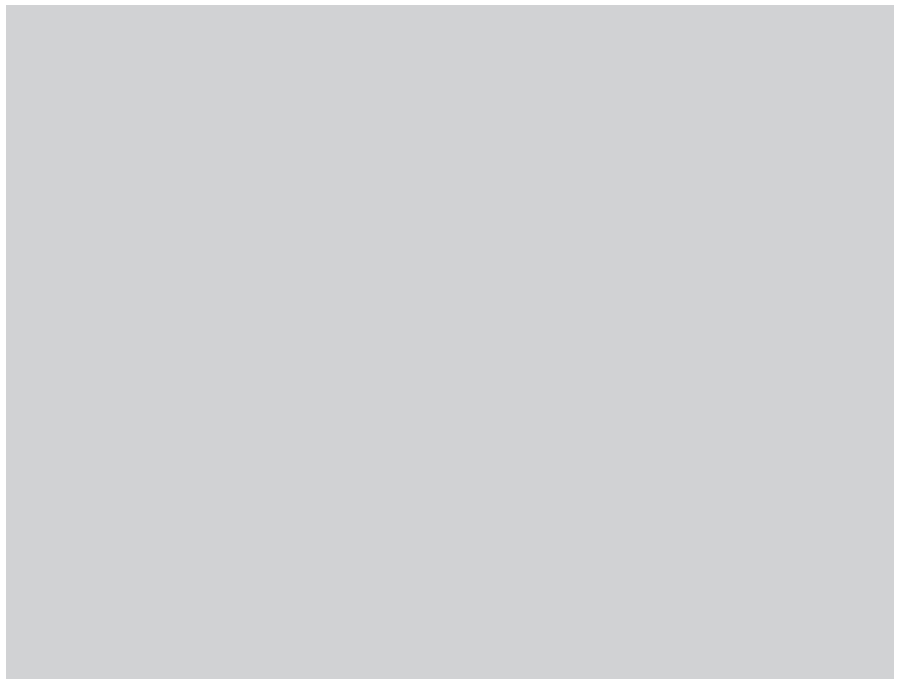
The precise nature of ductile fracture mechanisms in low triaxiality is still debated within the material science community. Experimental evidence²¹ shows that failure in shear strongly depends on the population of secondary particles. However, shear failure on the scale of dispersed grain-refining carbides is not well understood. Therefore, numerical simulations are used based on unit cell calculations as a tool to investigate these mechanisms. The first attempt was made in the context of a uniform periodic

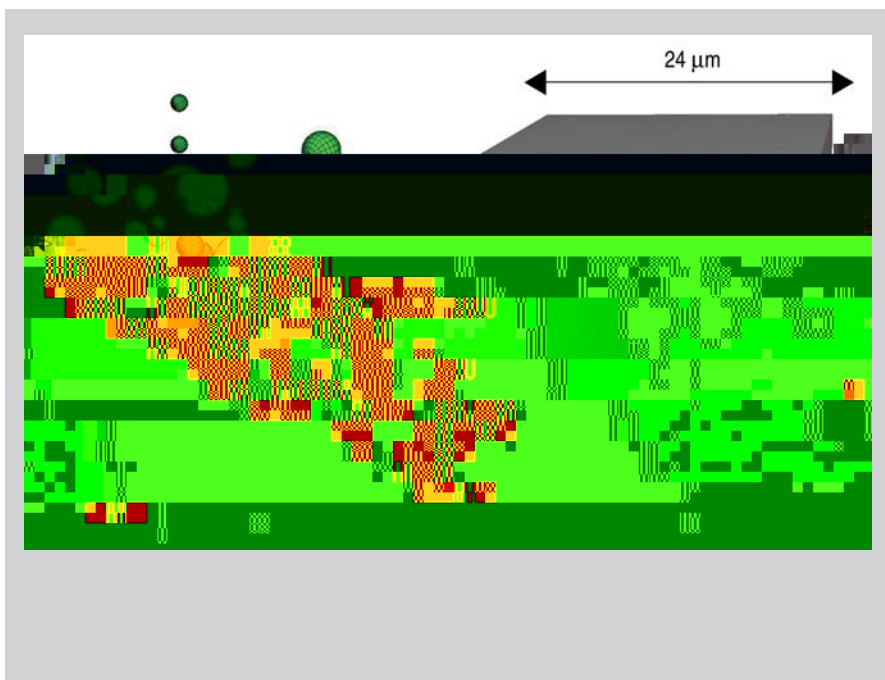
particle distribution using the unit cell depicted in Figure 3. After discretizing the cell with finite elements, one prescribes the cell to a state of pure shear strain (but zero net stress perpendicular to the shear plane) using periodic boundary conditions. In this example, the matrix material is linearly hardening and the volume fraction of the particle is 4%, well in excess of ~1%, the latter being a typical overall average volume fraction of such carbides (~0.5%). Figure 3 shows the effects of particle-matrix interface peak cohesive strength on the overall response of the cell. Three observations can be made. First, the debonding of the

particle triggers a steep softening in the stress-strain curve, but in this ideally dispersed microstructure the material recovers afterward. Second, the average debonding strain increases with the norm of the debonding peak stress, and third, after debonding, the material response converges with the response of the material with no bonding between the particles and the matrix. Therefore, although a softening event is observed during particle-matrix debonding, the resulting “transient” instability is confined to the local debonding event and thereafter the stress-strain curve continues to harden. In other words, no failure localization mechanisms could be obtained with this simplified particle configuration.

The effect of particle distribution was then investigated by simulating the shear deformation of a cluster of nine secondary particles with RVE volume fraction 2% and particle radii in the range 30–50 nm, as shown in Figure 4. In this computation, the matrix properties correspond to the 4330mod steel linear model (Table A). The average response of the cell is displayed in Figure 4. It is seen to exhibit a softening behavior due to material failure. This result accentuates the role of particle distribution on the failure of high-strength steel. The failure mechanism can be explained as a result of microvoid coalescence in a plane whose direction coincides with the shearing direction. After observation of Figure 4, one can note that in this plane, the top of one particle is aligned with the bottom of another







and the resulting compositional data set was discretized² into a set of ~12,000 carbide centroids and equivalent diameters. Voronoi tessellation of the centroids yielded 9,080 particles with complete nearest-neighbor tessellations, comprising an average particle volume fraction of 1.7%. In turn, the topology of the

